RSC Sustainability

ROYAL SOCIETY OF CHEMISTRY

PAPER

View Article Online
View Journal | View Issue

Cite this: *RSC Sustainability*, 2024, **2**, 1142

Revisiting the electrocatalytic hydrogenation of furfural to furfuryl alcohol using biomass-derived electrolytes†

Maria Wolfsgruber,[a] Robert H. Bischof,[b] Christian Paulik,[c] Adam Slabon *[de] and Bruno V. M. Rodrigues*[d]

Electrocatalytic hydrogenation of furfural to furfuryl alcohol represents a sustainable approach to utilizing renewable energy for producing bio-based platform chemicals. However, low Faraday efficiencies (FEs) and the use of organic solvents with high environmental impacts often render the process less sustainable than classical catalytic hydrogenation. In this study, we tested a two-compartment and three-electrode setup at ambient temperature and atmospheric pressure, featuring various electrodes (Ag, Au, CP, Cu, Pt, Sn, and a gold-coated silver wire (AucAg)), and biomass-derived electrolytes (acetic acid, levulinic acid, and sodium acetate). AucAg, serving as an electrocatalyst with 1 M sodium acetate as electrolyte, exhibited the best combination of FE and furfuryl alcohol yield with 79% and 35%, respectively. The optimum conditions were achieved at 100 rpm (stirrer speed) and −0.7 V *vs.* RHE. Scanning electron microscopy (SEM) and energy-dispersive spectroscopy (EDS) analyzes indicated no significant influence of the substances on the working electrode during the reaction. Since the identity of the cation of the electrolyte influences the electrode–electrolyte microenvironment, multiple alkali metals were trialed. Sodium ion as the counter ion emerged on top, surpassing potassium, and cesium ions for the electroreduction of furfural to furfuryl alcohol. This preference could be attributed to the competing hydrogen evolution reaction favored by Cs over K and Na. In this perspective, the highlights of a bioelectrorefinery concept for creating a bio-derived platform chemical in a sustainable solvent with green electrons are demonstrated and optimized.

Received 25th January 2024
Accepted 16th March 2024

DOI: 10.1039/d4su00040d

rsc.li/rscsus

Sustainability spotlight

In response to the challenges posed by traditional catalytic hydrogenation, the electrocatalytic conversion of furfural to furfuryl alcohol is revisited, aiming at overcoming obstacles like low Faraday efficiencies and the use of impactful organic solvents. By exploring various electrodes and biomass-based electrolytes, our work presents a sustainable avenue for harnessing renewable energy to produce bio-based chemicals. Aligned with the UN's SDG(s), specifically Goal 7 (Affordable and Clean Energy) and Goal 9 (Industry, Innovation, and Infrastructure), our work integrates green energy sources and environmentally benign electrolytes, reducing carbon footprints associated with traditional chemical production. While highlighting the importance of transitioning to eco-friendly methods, we emphasize the potential of bioelectrorefineries in fostering a sustainable future in the realm of chemistry and industrial processes.

Introduction

The achievement of global climate targets represents a necessary political and scientific commitment to our envrinoment.[1] To attain the goals of the European Climate Law and due to ecological, economic, and social factors, industry is endeavoring to make processes more sustainable.[2] The European Climate Law proposes climate neutrality by 2050 and a reduction of net greenhouse gas emissions by 55% from 1990 to 2030.[2] The use of biorefineries represents a major milestone as it promotes both the use of sustainable raw materials and the reduction of petroleum-based synthesis.[3,4] The compound annual growth rate (CAGR) for the biorefinery market is forecasted to be 8.2% by 2027, up from the global biorefinery market volume of USD 141.88 billion in 2022.[5] Furfural is one of the most promising platform chemicals obtained from biorefineries.[3] It is derived from lignocellulosic biomass and consists of a furan ring with an aldehyde group. The furfural

[a]*Kompetenzzentrum Holz GmbH, c/o Werkstraße 2, 4860 Lenzing, Austria*
[b]*Lenzing AG, Werkstraße 2, 4860 Lenzing, Austria*
[c]*Institute for Chemical Technology of Organic Materials, Johannes Kepler University, Altenberger Str. 69, 4040 Linz, Austria*
[d]*Chair of Inorganic Chemistry, University of Wuppertal, Gaußstraße 20, 42119 Wuppertal, Germany. E-mail: slabon@uni-wuppertal.de; manzolli@uni-wuppertal.de*
[e]*Wuppertal Center for Smart Materials & Systems, University of Wuppertal, 42119 Wuppertal, Germany*

† Electronic supplementary information (ESI) available. See DOI: https://doi.org/10.1039/d4su00040d

market volume was USD 556.74 million in 2022, with a projected increase to USD 900.84 million by 2030. Based on this, a CAGR of 6.20% is expected from 2023 to 2030.[6] Furfural finds applications in fungicides, insecticides, fertilizers, plastics, adhesives, manufacture inks, and flavoring compounds. Approximately 80% of the furfural is converted to furfuryl alcohol.[6] Furfuryl alcohol is used in resins and plastics, particularly in the production of furan resins for the metal casting industry as foundry sand binders.[7] The market value of furfuryl alcohol was USD 501 million in 2019, with a forecasted CAGR of 6.50% from 2021 to 2028.[8] Furfural is produced by acid-catalyzed conversion of xylan containing feedstocks. Xylan is depolymerized to xylose, and the xylose is subsequently dehydrated to form furfural.[9] Furfural is also obtained directly as a by-product of the pulp process in existing biorefineries, for example, at Lenzing AG.[10,11]

Commercially, two reduction pathways of furfural to furfuryl alcohol take place. On the one hand, a thermocatalyzed reduction reaction with gaseous H_2 as the hydrogen-donor occurs under pressures ranging from 20 to 50 bar and temperatures between 90–500 °C. Catalysts for the vapor-phase reactions includes copper, chromium, iron, zinc, bimetallic catalysts, *etc.*[12–14] The high pressure is needed to increase the solubility of hydrogen in the liquid phase. On the other hand, the Meerwein–Ponndorf–Verley reduction uses alcohol (*e.g.*, isopropanol) as hydrogen source with solid catalysts, *e.g.* metalorganic frameworks (MOFs) at temperatures around 140 °C.[15] Both variants involve costs associated with both elevated pressure and temperature, which also entail a considerable ecological footprint and safety concerns.[16] Additionally, catalysts like chromium and some solvents are toxic and pose safety issues. The large quantity of hydrogen gas is at present inevitably accompanied with high economic and ecological costs, and accounts for a major proportion of the overall operating costs. The latter can be for hydrogen ten times higher due to transport and storage, which, in turn, is important for remote biorefinery plants located in the vicinity of cheaply available biomass.[17,18]

Electrocatalytic hydrogenation emerges as a sustainable and more selective approach for biomass valorization. Unlike traditional hydrogenation methods, electrocatalytic hydrogenation does not require an external hydrogen-donor source, as hydrogen is generated *in situ* at the cathode. It operates at room temperatures and atmospheric pressures, utilizing aqueous solvents. When combined with green energies such as solar and wind energy, and renewable raw materials, electrocatalytic hydrogenation becomes a more ambitious and environmentally friendly approach.[1,3,19–22] The mechanism of the electrocatalytic hydrogenation of furfural to furfuryl alcohol has been recently studied by Chadderdon *et al.* and also Liu *et al.*[23,24] Liu *et al.* proposed that the carbonyl group of the furfural adsorbs onto the electrocatalyst surface, forming a carbon radical with a proton. The secondary carbon radical interacts with adsorbed hydrogen to produce furfuryl alcohol. The adsorbed hydrogen is electrochemically produced during water reduction. The final step involves desorption of the furfuryl alcohol from the electrocatalytic surface. The rate-determining step in this reaction is the first addition of the proton and the formation of the radical.[24]

Several experimental studies have explored the electrochemical reduction of furfural to furfuryl alcohol, which have been summarized and detailed discussed in the ESI (Table S1†). Zhao *et al.* investigated the electrocatalytic hydrogenation of furfural to furfuryl alcohol using copper, nickel, lead, and platinum (Pt) supported on carbon fibers. Different electrolytes, including H_2SO_4, HCl, $HClO_4$, and NaOH were tested. The most favorable results could be obtained with 3% Pt on activated carbon fibers in 0.1 M HCl, achieving a yield of approximately 85% and a Faraday efficiency (FE) of nearly 85% at 50 °C. It is noteworthy that this setup was operated at an elevated temperature, and after reusing the electrode, a slight decrease in both yield and FE was observed.[25] It is essential to highlight that Pt, as an electrocatalytic active material, carries a high ecological footprint in term of CO_2 equivalents, with 69 410 tCO_2 equivalent per ton of platinum.[26] In comparison, silver (Ag) was reported to have a CO_2 factor of 449, and gold (Au) was reported to have a factor of 47 790 tCO_2 equivalent per ton.[26] The preparation of the Pt-supported activated carbon fiber electrodes is a complex procedure, and with pure Pt, only a conversion of 5% could be achieved.[25] Other complex electrocatalysts, such as La-doped TiO_2, were also tested. This process, used in combination with DMF as a solvent and tetra-butyl-ammonium bromide as a mediator, achieved high yields of 86% and FE of 89%. However, the use of these solvents and mediators makes the process less environmentally friendly and sustainable.[27]

Cao *et al.* reported on the use of a microchannel flow reactor for the electrocatalytic reduction of furfural to furfuryl alcohol. For the flow reactor type, a mixture of ethanol and water was used as solvent system along with potassium ethylate as electrolyte. Both, the yield and the FE, had values around 90%.[28] From an ecological and process safety perspective, however, ethanol has higher associated CO_2 emissions than water as a solvent, while potassium ethylate is flammable, corrosive, and reacts vigorously with water.[26,29] Furthermore, electrode pollution necessitating a cleaning step was observed.[28] Other setups with nickel, copper, graphite, stainless steel, palladium, iron, and various electrodes, often in organic solvents and with mediators, have been explored for the conversion of furfural to furfuryl alcohol.[30–34] Many of these electrodes materials have high CO_2 factors, and their activity and stability are significantly influenced by the reaction.[26,30–34] In addition, substantial efforts are invested in the production and surface optimization of many variants of catalysts, incurring high costs. Furthermore, the use of organic solvents and mediators in many processes is less sustainable compared to aqueous solutions.[30–34] Overall, processes could become more sustainable and environmentally friendly by replacing certain chemicals or solvents. For instance, greener electrolytes like acetic acid or levulinic acid, producible in biorefineries, could be employed. In the pulp and paper industry, extracted acetic acid can be utilized, converted into sodium acetate using the sodium hydroxide solution already present for fiber processes in the pulp and paper industry.[35] Post-reaction, the electrolyte can be reused or separated through the application of bipolar membranes and electrodialysis.[36–38]

For numerous electrocatalytic processes, extensive research has explored cation effects of the electrolyte on electrochemical reduction.[39–43] The three primary theories regarding cation effects on electrocatalytic reduction are: modification of the local electric field, stabilization of intermediates, and buffering of pH. Particularly, the hydration shells of cations significantly impact their activity. In the reduction of CO_2 on Ag and Cu electrocatalysts, the cation activity follows the order Cs > K > Na.[40,41] Cs, with the smallest hydrated cation radius, leads to higher cation concentrations on the electrode–electrolyte interface, resulting in a higher surface charge density and a stronger electric field.[40] The cation effect on the hydrogen evolution reaction (HER) on Pt contrasts with CO_2 reduction, with the activity order of Na > K > Cs.[39] For the HER on Au and Ag as electrocatalytic materials, the activity order is Cs > K > Na. Xue *et al.* suggested that this effect is due to the change in the H-binding energy on the electrode surface due to presence of cations.[39]

Electrocatalytic processes in biorefineries hold significant potential for sustainable and green biomass valorization. The electrocatalytic reduction of furfural to furfuryl alcohol has been explored in previous studies. Our here reported setup, utilizing electrolytes based on renewable raw materials and water as

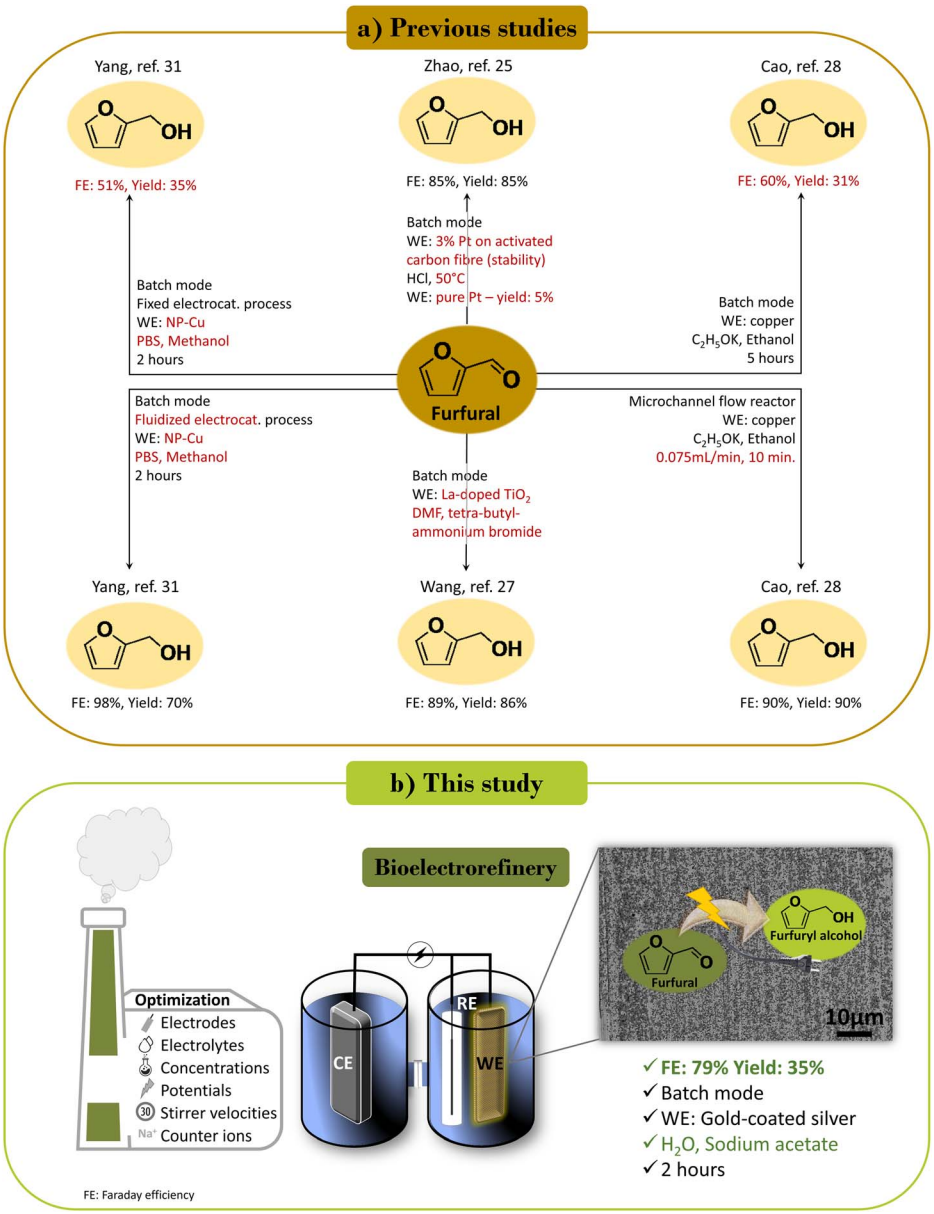

Scheme 1 (a) Summary of representative previous works of the electrochemical reduction of furfural to furfuryl alcohol and their drawbacks marked in red. (b) Schematic illustration of the electrocatalytic hydrogenation of furfural to furfuryl alcohol using a membrane cell. The system consists of a three-electrode setup (WE: working electrode, CE: counter electrode, RE: reference electrode) with varied aqueous electrolytes and multiple WEs (silver, gold, gold-coated silver, carbon paper, copper, tin, and platinum). Optimization related to electrodes and electrolytes, electrolyte concentrations, potential dependence, stirrer speed, and different counter ions are presented. This electrocatalytic reduction in biorefineries can be industrial embedded as *bioelectrorefinery*.

a solvent, stands out from previous reports, because the latter rely on organic solvents with toxic mediator systems. We provided a systematic study using various electrocatalysts with different electrolytes and investigated the influence of alkali metal cations on the activity of the reduction reaction. Our investigation represents a direct approach on the valorization of furfural into the high value-added product furfuryl alcohol, adhering to the principles of *Green Chemistry* (Scheme 1).

Experimental

Materials

Silver wire (Ag, 1.0 mm, 99.9%), platinum wire (Pt, 1.0 mm, 99.95%), and gold wire (Au, 0.5 mm, 99.95%) were purchased form abcr GmbH. The platinum gauze (52 mesh woven 0.1 mm, 99.9%, 25 × 25 mm^2) was acquired from Alfa Aesar. Tin wire (Sn, 1.0 mm, 99.998%), toray carbon paper (CP, TGP-H-60), levulinic acid (LA, >98%), cesium acetate (CsAc, >97%), and potassium acetate (KAc, 99%) were purchased from Thermo Scientific. Copper foil (Cu, thickness 0.025 mm, 99.98%) and sodium acetate (NaAc) trihydrate (p.a.) were acquired from Sigma-Aldrich. Fumapem F-10100 cation exchange membrane was purchased from Fumatech BWT GmbH, whereas tetrachlorauric(iii) acid ($HAuCl_4$) was acquired from Acros Organics. Sulfuric acid (H_2SO_4, 95%) was purchased from VWR. Furfural (FF, >99.9%) and acetic acid (HAc, >99.9%) were provided by the Lenzing AG. DI water and Milli-Q water were used for all experiments. The Potentiostat was a Gamry Interface 5000E.

Solutions

The FF concentration in the catholyte chamber of the H-cell experiments was 0.1 mol L^{-1} (M) for all experiments. LA, NaAc, HAc, KAc, and CsAc were used as electrolytes. The electrolyte concentrations varied from 0.1 to 4.0 M. All electrolytes were dissolved in Milli-Q water and then FF was added. Electrolyte solutions without FF were used in the anolyte chamber. The solutions for all experiments, along with the concentrations of the chemicals, are listed in Table 1.

Table 1 Summary of the solutions for the experiments, including the abbreviation of each solution, the concentration of furfural (FF) *c*(FF) the chosen electrolyte and the electrolyte concentration *c*(E) with the corresponding pH value of the solution. The electrolytes levulinic acid (LA), acetic acid (HAc), sodium acetate (NaAc), potassium acetate (KAc), and cesium acetate (CsAc) were used

Name	*c*(FF)/ mol L^{-1}	Electrolyte	*c*(E)/ mol L^{-1}	pH
LA + FF	0.1	Levulinic acid (LA)	0.1	3.0
LA	—	Levulinic acid	0.1	3.0
HAc + FF	0.1	Acetic acid (HAc)	0.1	2.9
HAc	—	Acetic acid	0.1	2.9
NaAc + FF	0.1	Sodium acetate (NaAc)	0.1	8.5
NaAc	—	Sodium acetate	0.1	8.5
1NaAc + FF	0.1	Sodium acetate	1.0	8.7
1NaAc	—	Sodium acetate	1.0	8.7
2NaAc + FF	0.1	Sodium acetate	2.0	8.9
2NaAc	—	Sodium acetate	2.0	8.9
3NaAc + FF	0.1	Sodium acetate	3.0	9.1
3NaAc	—	Sodium acetate	3.0	9.1
4NaAc + FF	0.1	Sodium acetate	4.0	9.3
4NaAc	—	Sodium acetate	4.0	9.3
1KAc + FF	0.1	Potassium acetate (KAc)	1.0	7.9
1KAc	—	Potassium acetate	1.0	7.9
4KAc + FF	0.1	Potassium acetate	4.0	8.7
4KAc	—	Potassium acetate	4.0	8.7
1CsAc + FF	0.1	Cesium acetate (CsAc)	1.0	6.5
1CsAc	—	Cesium acetate	1.0	6.5
4CsAc + FF	0.1	Cesium acetate	4.0	7.1
4CsAc	—	Cesium acetate	4.0	7.1

Electrocatalysis

Ag, Au, CP, Cu, Pt, Sn, and a gold-coated silver wire (AucAg) were used as working electrodes (WE) in a three-electrode setup. AucAg was prepared accordingly to previous studies from our group.[20,44] For all experiments, a Pt mesh was used as counter electrode (CE) and an Ag/AgCl (saturated KCl) as reference electrode (RE). The measured potentials *vs.* Ag/AgCl (saturated KCl) were converted *vs.* RHE according to the following eqn (1):

$$E_{RHE} = E^0_{Ag/AgCl(sat.\ KCl)} + 0.059pH + E_{Ag/AgCl(sat.\ KCl)} \quad (1)$$

where $E^0_{Ag/AgCl(sat.\ KCl)}$ is the potential of Ag/AgCl (saturated KCl) *versus* standard hydrogen electrode with 0.197 V.[45] $E_{Ag/AgCl(sat.\ KCl)}$ is the observed potential during the experiment and pH is the pH value of the solution in the catholyte chamber. The electrocatalytic reactions were performed in a membrane cell (H-cell) with 50 mL chambers. The pretreatments of the electrodes and the membranes were in line with our previous studies.[20,44] Linear sweep voltammetry (LSV) experiments with the aforementioned WEs with the electrolytes LA, HAc and NaAc to test the inter-combinations of WEs and electrolytes were performed. An electrode surface of 1 cm^2 was selected. For each WE in combination with the three electrolytes, a LSV curve was obtained with furfural (FF) in the solutions (LA + FF, HAc + FF, NaAc + FF) and without FF (LA, HAc, NaAc) in the catholyte chamber. Differences in the reaction behavior should be recognizable, indicating a reaction with FF. The chronoamperometric (CA) experiments were determined based on the results obtained from the LSV curves. A detailed summary of all CA experiments can be found in Table S2.† The reaction time of the preliminary CA experiments was 2 h, and the stirrer speed was set at 200 rpm. LA, as an electrolyte, was tested in combination with Ag (−0.6 V *vs.* RHE), Sn (−0.9 V *vs.* RHE), and CP (−0.9 V *vs.* RHE) as WEs. Combinations of HAc as an electrolyte and Ag (−0.6 V *vs.* RHE), Sn (−0.9 V *vs.* RHE), CP (−1.0 V *vs.* RHE), AucAg (−0.6 V *vs.* RHE), and Au (−0.6 V *vs.* RHE) as WEs were explored. Experiments with the electrolyte NaAc were carried out with Ag (−0.5 V and −0.7 V *vs.* RHE), Sn (−1.1 V and −0.7 V *vs.* RHE), AucAg (−0.7 V *vs.* RHE), CP (−0.7 V and −1.0 V *vs.* RHE), and Au (−1.0 V *vs.* RHE) as WEs. Based on the CA preliminary experiments, the system with NaAc as electrolyte and AucAg as the WE was selected for the optimization tests. The NaAc concentration for the system with AucAg was increased to 1 M, and a potential screening with the potentials

−0.5 V, −0.6 V, −0.7 V, −0.8 V, −0.9, −1.0, −1.1, −1.2 and −1.3 V *vs.* RHE was performed. The reaction time was again set to 2 h and the stirrer speed at 200 rpm. The best Faraday efficiency (FE) was observed at −0.7 V *vs.* RHE, and the influence of the electrolyte concentration was determined. Therefore, NaAc concentrations of 1, 2, 3, and 4 M were tested under the same experimental conditions. After achieving the highest FE with a NaAc concentration of 4 M, the stirrer speed was varied between 0 and 1000 rpm. The optimal FE was observed at 100 rpm. All subsequent experiments were performed with a stirrer speed of 100 rpm. The influence of the counter ions of the electrolyte was investigated through experiments using 1 M and 4 M KAc, and 1 and 4 M CsAc as electrolytes, along with 0.1 M FF. The experiments had a reaction time of 2 h, a stirrer speed of 100 rpm, and a 1 cm^2 AucAg WE. Afterwards the geometric surface area of the AucAg WE was increased to 4 and 8 cm^2. Four experiments were conducted, each with a reaction time of 2 h, a stirrer speed of 100 rpm, and a potential of −0.7 V *vs.* RHE. The first and the second experiments, using the two different electrode sizes, were performed with a NaAc concentration of 1 M as the electrolyte, while the third and the fourth experiments, corresponding to the two electrode sizes, were conducted with a 4 M NaAc concentration. The experiment yielding the optimal outcome under the most promising conditions was subsequently replicated three times to assess the repeatability of the results.

Characterization

The quantification of furfural and furfuryl alcohol was performed using reversed-phase chromatography combined with UV detection. A Thermo Scientific ICS 5000+ high performance liquid chromatography (HPLC) system, equipped with a Dionex UVD 340 detector and a Thermo BDS Hypersil C8 250 × 4.6 mm 5μ separation column, was used. A Goebel S5200 autosampler and a Dionex P680 pump were applied. For isocratic elution, a flow rate of 1 mL min^{-1} with a mixture of water and acetonitrile was used. A two-point calibration for both substances with 1 and 10 mg L^{-1} was performed. The injection volume was 20 μL. The UV detection for furfuryl alcohol was carried out at 216 nm and for FF at 277 nm. A Thermo Fisher Quanta 450 was used to analyze the morphology of the WEs *via* Scanning Electronic Microscopy (SEM). The accelerating voltage was set to 10 kV. The topography of the electrodes was analyzed using energy-dispersive spectroscopy (EDS) with an accelerating voltage of 15 kV on the Phenom pro XL.

Results and discussion

Linear sweep voltammetry (LSV)

The experiments for the LSV curves were all conducted in a two-compartment cell with a Pt mesh CE and an Ag/AgCl (saturated KCl) RE. The catholyte chamber contained FF and an electrolyte concentration of 0.1 M. The anolyte compartment had an electrolyte concentration of 0.1 M. HAc, NaAc, and LA were chosen as electrolytes. All WEs had a geometric surface area of 1 cm^2, and the materials Ag, Au, CP, Cu, Pt, Sn, and AucAg were tested as electrocatalytic materials with every electrolyte. To define a selection of suitable electrolyte-WE-combinations, a second set of LSV experiments was performed using only the electrolytes (without FF in the catholyte chamber). For the LSV curves, attention was given to the differences between the curves for the same electrode–electrolyte setup with and without FF. The emphasis was on analyzing the shape of the curves and the onset potentials. Additionally, comparisons were drawn with electrochemical reductions reported in other literature. The collective findings were utilized to determine the electrode–electrolyte combinations for the subsequent CA tests. The onset potentials are displayed in Table 2, and the corresponding LSV curves are presented in the ESI,† including also a more detailed discussion (Fig. S1–S3†). The onset potential for the reduction reactions with NaAc as the electrolyte was determined as the difference of 0.01 mA cm^{-2} per 1 mV. Among the various WEs with NaAc as the electrolyte and FF, the order of onset potentials was C > Cu > Sn > Au > Ag > AucAg > Pt, with the most cathodic one at the beginning. Notably, for the Ag electrocatalyst, the onset potential without FF was approximately 0.4 V more cathodic than with FF. FF in combination with Sn as the WE had twice the onset potential compared to without FF.

Table 2 Summary of the LSV experiments with different types of working electrodes (silver, gold, gold-coated silver, carbon paper, copper, platinum, tin), all having a geometric surface area of 1 cm^2. The three electrolytes sodium acetate, levulinic acid, and acetic acid were used. All experiments were performed in an H-cell with a three-electrode setup with a platinum mesh as CE and an Ag/AgCl (KCl saturated) RE. The onset potentials with the electrolytes and furfural ($E_{on\text{-}set}$(FF)) in the catholyte solution and only with the electrolytes ($E_{on\text{-}set}$(E)) are listed

	$E_{on\text{-}set}$(FF)/ V *vs.* RHE	$E_{on\text{-}set}$(E)/ V *vs.* RHE
Sodium acetate		
Silver	−0.54	−0.97
Gold	−0.61	−0.80
Gold-coated silver	−0.48	−0.91
Carbon paper	−0.70	−1.14
Copper	−0.69	−0.78
Platinum	−0.28	−0.24
Tin	−0.62	−1.14
Acetic acid		
Silver	−0.43	−0.59
Gold	−0.29	−0.30
Gold-coated silver	−0.36	−0.36
Carbon paper	−0.61	−0.79
Copper	−0.59	−0.59
Platinum	−0.12	−0.06
Tin	−0.87	−0.98
Levulinic acid		
Silver	−0.38	−0.46
Gold	−0.24	−0.25
Gold-coated silver	−0.32	−0.29
Carbon paper	−0.62	−0.68
Copper	−0.42	−0.47
Platinum	−0.09	−0.03
Tin	−0.57	−0.63

With AucAg, the onset potential of the reduction reactions decreased in the presence of FF from −0.91 V to −0.48 V *vs.* RHE. For CP, not only did the onset potential differ by −0.5 V, but the gradient of the LSV curve with FF was also steeper. In the case of Au, the slope of the LSV curve was steeper with FF than without FF, and a difference in the onset potential was also determined. Therefore, the combinations of Ag, Au, AucAg, CP, and Sn in combination with NaAc as electrolyte were selected for CA experiments. For Pt and NaAc as the electrolyte, very similar LSV curves with and without FF were observed. Hydrogen evolution was noticeable at very low cathodic potentials. Based on these findings, it was not chosen for further experiments. Similarly, no additional tests were conducted due to the analogous results observed for Cu.

With HAc and LA as electrolytes and FF in the solution, the onset potentials were determined at a slope of 0.001 mA cm^{-2} per 1 mV. For HAc as electrolyte, the order of the onset potential was Sn > C > Cu > Ag > AucAg > Au > Pt. Ag, Au, AucAg, CP, and Sn were chosen for further CA experiments with HAc as the electrolyte. In general, for HAc as the electrolyte with different WEs, the onset potentials with and without FF had smaller differences. For Ag as the WE, the onset potential without FF was −0.59 V *vs.* RHE and with FF −0.43 V *vs.* RHE. AucAg exhibited a sharper LSV curve with FF than without FF. For Au as the WE, the shapes of the LSV curves differed. Au and AucAg had very similar onset potentials with and without FF. Due to the curve shapes and also based on some literature research, these WEs were also chosen for further CA experiments.[20,33,46] The difference in the onset potentials with Sn in combination with and without FF was 0.1 V, and for CP, it was nearly 0.2 V. Pt and Cu were not selected for further experiments due to the visually visible HER and the very similar onset potentials. Pt is also known for its very strong HER development, as reported in the literature.[47]

For LA as the electrolyte, the order of the on-set potentials was C > Sn > Cu > Ag > AucAg > Au > Pt. In this case, only Ag, Sn, and CP were tested for further CA experiments. Ag was chosen because of the difference in the onset potentials with and without FF and due to the steeper LSV curve with FF. Sn had a less cathodic onset potential with FF than without FF. The slope of the LSV curve with FF was sharper than without FF for CP. The onset potentials for Au, AucAg, Cu, and Pt were very similar with and without FF. For all three different electrolytes, the less cathodic onset potential was observed for Pt as the WE. C, Cu, and Sn as WEs had the most cathodic onset potentials, while Ag, AucAg, and Au were in between.

Chronoamperometry (CA)

All CA experiments had a reaction time of 2 h and were conducted in an H-cell with a Pt mesh as the CE and an Ag/AgCl (saturated KCl) RE. The initial and final FF concentrations, the FEs, and the furfuryl alcohol yields for all CA experiments are listed in Table S3.† The FE and the furfuryl alcohol yield were calculated according to eqn (1) and (2) in the ESI.† With LA as the electrolyte and Ag as the WE at a potential of −0.6 V *vs.* RHE, a yield of 0.07% furfuryl alcohol with a FE of 15% was achieved. Sn and CP were also tested as electrocatalysts, both at −0.9 V *vs.* RHE, but no conversion of FF to furfuryl alcohol could be achieved for these materials. The CA experiments for the conversion of FF to furfuryl alcohol with HAc as electrolyte were performed with Ag, Sn CP, AucAg, and Au as electrochemically active materials. Sn and CP as WEs showed no turnover. The experiments with Ag, AucAg, and Au as WEs were performed at −0.6 V *vs.* RHE. For Ag with HAc as the electrolyte the yield of furfuryl alcohol and the FE were nearly the same as for LA as the electrolyte. For AucAg and Au, the yields increased to 0.10 and 0.17%, with FEs of 17 and 26%, respectively. With NaAc as the electrolyte and AucAg as electrocatalytic material, a yield of 1.0% with a FE of 20% was reached. With Ag as WE, approximately a quarter of the yield could be achieved. Twice as much furfuryl alcohol could be produced with Au compared to Ag. The yield of furfuryl alcohol with Sn was less than 1‰, and no conversion of FF to furfuryl alcohol could be achieved with CP. Due to the best values for the combination of yield and FE, the system with NaAc as the electrolyte and AucAg as the WE was used for further optimization.

To enhance the current density of the system, the electrolyte concentration was increased from 0.1 to 1.0 mol L^{-1}. At a potential of −0.7 V *vs.* RHE, the yield increased from 1.0 to 6.0%, and the FE improved from 20 to 58%. To determine the potential with the highest reaction rate of FF to furfuryl alcohol, a potential screening between −0.5 and −1.3 V *vs.* RHE was conducted. Fig. 1 illustrates the FE and the yield (*Y*) of furfuryl alcohol *versus* the different reaction potentials. The CA experiments were performed in an H-cell with 0.1 M FF and 1.0 M FF over a reaction time of 2 h. The optimal combination of FE and yield of furfuryl alcohol was achieved at −0.7 V *vs.* RH, where the FE was 58% and the yield of furfuryl alcohol reached 6%. The decrease in FE at more cathodic potentials could be attributed to the dominance of the HER and side-products formation.[16,23,30,48]

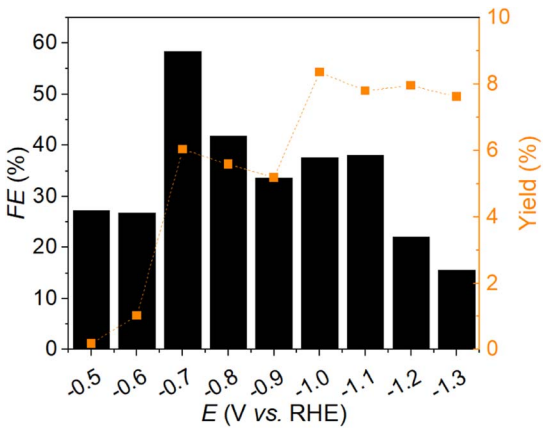

Fig. 1 Faraday efficiency (FE) and the furfuryl alcohol yield (*Y*) *versus* different potentials (−0.5, −0.6, −0.7, −0.8, −0.9, −1.0, −1.1, −1.2 and −1.3 V *vs.* RHE) of the CA experiments. The reactions were performed in an H-cell with a three-electrode setup with Au-coated Ag as the WE, platinum as the CE and Ag/AgCl (saturated KCl) as the RE. The geometric surface area of the WE was 1 cm^2, and the reaction was conducted in a solution with 0.1 M furfural and 1.0 M sodium acetate over a reaction time of 2 h (pH 8.7).

The potential in the less cathodic region was insufficient to overcome the activation energy for the reduction of furfural to furfuryl alcohol. The recurring drops may indicate the presence of by-products, with one possibility being the electrodimerization reaction to hydrofuroin published by Dhawan *et al.*[16] The electrocatalytic hydrogenation of FF is always in competition with the direct electroreduction, making the selective electrocatalytic reduction of FF challenging.[23,30,48]

At more cathodic potentials, the yield was higher, however, due to the low FE and the associated loss in energy, the sustainability and economic efficiency of the system would be jeopardized.[1,40,49]

After finding the most suitable reaction potential at −0.7 V *vs.* RHE for the reduction of FF to furfuryl alcohol, the electrolyte concentration was also tested. Reactions with 0.1, 1.0, 2.0, 3.0 and 4.0 M NaAc were used for the optimization and tested at the previously determined potential. The FF concentration was 0.1 M for all experiments and the reaction time was set to two hours. An H-cell with the AucAg WE with a geometric surface area of 1 cm^2 was used. The FEs and furfuryl alcohol yields can be found in Fig. 2. The highest electrolyte concentration resulted in the best FE with 75%. The furfuryl alcohol yield of this reaction was 3.7%. The highest furfuryl alcohol yield with 6.0% was achieved with an electrolyte concentration of 1.0 M NaAc. The FE of this reaction was nearly 60%. It is known, that the activity of a electrochemical reaction has its optimum at a defined electrolyte concentration.[50] The higher NaAc concentration could limit the mobility of the ions, since the ions can hinder each other by virtue of mutual attraction. Another possible reason could be that more diluted solutions contain higher proportions of oxonium ions, which means better current conduction.[51] Visually, accumulating HER gas bubbles could also be seen at higher electrolyte concentrations. One possibility for reducing the yield is that the presence of the accumulating gas bubbles interferes with the current flow and the electrode-substrate interphase. This effect was previously studied by Sun *et al.*[52] The liquid conductivity of the membrane cell system could also decrease due to the fact, that the acetate ions cannot pass the cation exchange membrane.[52] Based on the results of these experiments further tests were performed with electrolyte concentrations of 1.0 and 4.0 M NaAc, because high yields could be achieved with 1.0 M NaAc and the high FEs with 4.0 M NaAc.

To determine the influence of the stirrer speed on the reduction reaction of FF to furfuryl alcohol, CA experiments without stirring and with 100, 200, 400, 600, 800 and 1000 rpm were performed (Fig. 3). The reaction setup was in the H-cell with 4.0 M NaAc as electrolyte and 0.1 M FF. The 4.0 M NaAc solution was chosen due to the high FE in the previous project. A three-electrode setup with an AucAg WE with a geometric surface area of 1 cm^2, Pt mesh as CE and Ag/AgCl (saturated KCl) as RE. The highest FE was achieved at 100 rpm and decreased with higher stirrer speeds. The maximum of the furfuryl alcohol yield was at 400 rpm and decreased with higher and lower stirring speeds.

Without stirring, the mass-transport to the electrocatalytic interface could not be granted. A larger proportion of the current went into the by-products at higher stirring speeds. These behaviours could be an indicator that the reaction is not diffusion-controlled and mass transport limited.[53] Another possibility is that side-reactions are preferred at higher stirrer speeds, like the HER.

To assess the influence of electrolyte counter ions on the reaction rate in the conversion of furfural to furfuryl alcohol, experiments were conducted with Na^+, K^+, and Cs^{2+}. Building upon the study with varying electrolyte concentrations, experiments were conducted at concentrations of 1.0 and 4.0 M. NaAc, KAc, and CsAc were tested as electrolytes in an H-cell over a 2 h reaction time. Pt served as the counter electrode (CE), and Ag/AgCl (saturated KCl) as the reference electrode (RE). Fig. 4 illustrates the Faraday efficiency (FE) and furfuryl alcohol yield

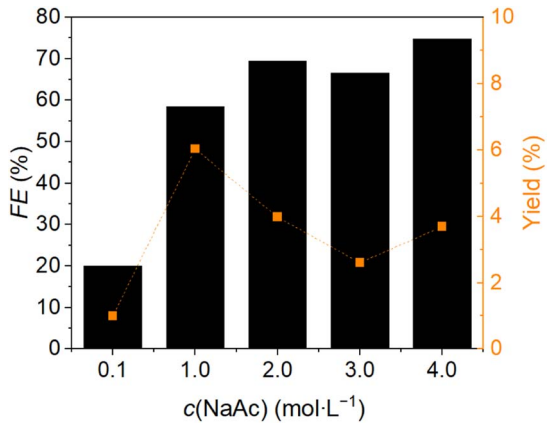

Fig. 2 Faraday efficiency (FE) and furfuryl alcohol yield (*Y*) *versus* the electrolyte concentrations (*c*(NaAc)) with 0.1 M (8.5), 1 M (pH 8.7), 2 M (pH 8.9), 3 M (pH 9.1), and 4 M (pH 9.3) NaAc and 0.1 M furfural. In the H-cell a three-electrode setup of Au-coated Ag with a geometric surface area of 1 cm^2, platinum, and Ag/AgCl (saturated KCl) was used as WE, CE and RE, respectively. The reaction time was two hours and the reaction potential −0.7 V *vs.* RHE.

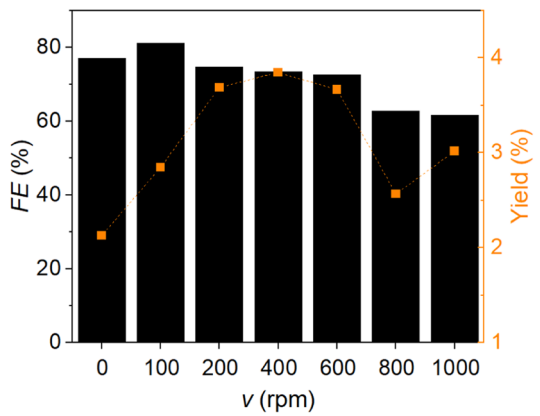

Fig. 3 Dependence of the Faraday efficiency (FE) and the furfuryl alcohol yield (*Y*) *versus* the stirrer speed in the H-cell. The NaAc concentration was 4.0 M and the furfural concentration 0.1 M, respectively. An AucAg WE, platinum CE and Ag/AgCl (saturated KCl) RE electrode were used within a reaction time of two hours. The reaction potential was −0.7 V *vs.* RHE (pH 9.3).

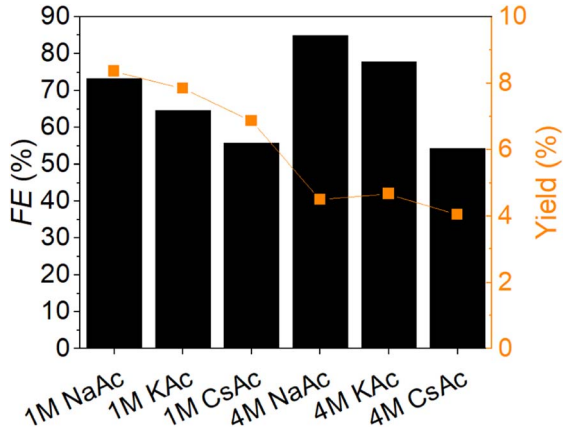

Fig. 4 Influence of different electrolyte counter ions on the Faraday efficiency (FE) and the furfuryl alcohol yield (*Y*). As electrolytes, sodium acetate (NaAc), potassium acetate (KAc), and cesium acetate (CsAc) were tested at concentrations of 1.0 and 4.0 M. Furfural concentration was 0.1 M in the H-cell and the reaction time 2 h at −0.7 V *vs.* RHE for NaAc and KAc and −0.8 V *vs.* RHE for CsAc. The WE was AucAg with a geometric surface area of 1 cm^2, the CE was a platinum mesh, and the RE was Ag/AgCl (saturated KCl).

concerning different electrolytes and their respective concentrations. The significant impact of various cations on the reaction aligns with findings from previous studies.[40,54] At an electrolyte concentration of 1.0 M, the FE and the furfuryl alcohol yield exhibited an activity trend of Na > K > Cs. This trend contrasts with many electroreduction studies focused on CO_2.[40,42] Numerous studies have explored the impact of counter ions in the electrolyte on reaction activity, yielding controversial findings. For HER on Pt, Xue *et al.* reported an activity trend of Na > K > Cs, consistent with our study presented here. However, in their studies on Au and Ag, the trend was reversed.[39] The observed preference for Na > K > Cs in our study may be attributed to the fact that HER, a competing reaction, is better facilitated by Cs than Na, as indicated in Xue *et al.*'s studies.[39] In the reduction of FF to furfuryl alcohol, HER is an unwanted side-reaction and is less favoured with Na^+ on Au and Ag electrodes.[39] The primary theories concerning the microenvironmental effect of cations include the influence of the local electric field, stabilization of the reaction intermediates, and pH dependency, in combination with the hydration shells and the hydration energy.[40,42,54] At a 1.0 M NaAc concentration, the highest furfuryl alcohol yield exceeded 8%, with over 70% of the current directed toward the reduction of FF. At a 1.0 M electrolyte concentration, K^+ as a counter ion achieved a FE of 65%, while Cs^{2+} reached 56%. The furfuryl alcohol yields were below 8% for K^+ and below 7% for Cs^{2+}. At a 4.0 M NaAc concentration, the yield was half compared to 1.0 M NaAc, but the FE was 10% higher. The FEs of the reactions at 4.0 M electrolyte concentration followed the order Na > K > Cs, similar to the 1.0 M concentration. The furfuryl alcohol yield for Na^+ and K^+ as counter ions was around 4.5%, while for Cs^{2+}, it was at 4.0%.

As NaAc emerged as the preferred electrolyte from experiments with various counter ions, additional experiments were conducted with 1.0 M and 4.0 M NaAc electrolytes using enlarged AucAg WE surface. The H-cell contained 0.1 M FF, with Ag/AgCl (saturated KCl) as the RE and Pt as the CE. The reaction time was 2 h. Fig. 5 illustrates the FE and furfuryl alcohol yield in relation to the different geometric WE surface (1, 4, and 8 cm^2) and electrolyte concentrations (1.0 and 4.0 M NaAc). The furfuryl alcohol yield decreased for all three surface sizes from 1.0 to 4.0 M concentration, while the FEs increased. Increasing the WE size resulted in an enhanced conversion rate. The highest furfuryl alcohol yield reached 37% with a geometric surface area of 8 cm^2 and a NaAc concentration of 1.0 M, with a corresponding FE of 82%. With the same electrolyte concentration, a yield of 18% could be achieved with 4 cm^2 and a yield of 8% with 1 cm^2. With a NaAc concentration of 4.0 M, furfuryl alcohol yields were 3%, 12%, and 19% for the geometric surface areas of 1 cm^2, 4 cm^2, and 8 cm^2, respectively, accompanied by corresponding FEs of 71% and 73%. These results align with findings previously published by Gil-Carrera *et al.*[55] After determining the optimal reaction conditions, the experiment's repeatability was assessed by conducting the reaction three times. The average yield of furfuryl alcohol was found to be 35.3% with a standard deviation of 3.1%, while the average faradaic efficiency (FE) was calculated to be 79% with a standard deviation of 7%.

SEM and EDS measurements were conducted to assess the stability of the working electrode and the impact of the reaction on the electrode surface. SEM micrographs of the WE before (Fig. 6a) and after (Fig. 6b) the reaction were analyzed to detect any changes in the morphology of the WE surface. No significant influence of the reduction reaction of FF to furfuryl alcohol could be observed on the micrographs of the AucAg WE. For this analysis, the optimal experimental conditions were employed, including 1.0 M NaAc, 0.1 M FF, an H-cell, and a reaction time of 2 h. AucAg with a geometric surface area of 8 cm^2 was used as the WE, Pt as CE, and Ag/AgCl (saturated KCl) as the RE.

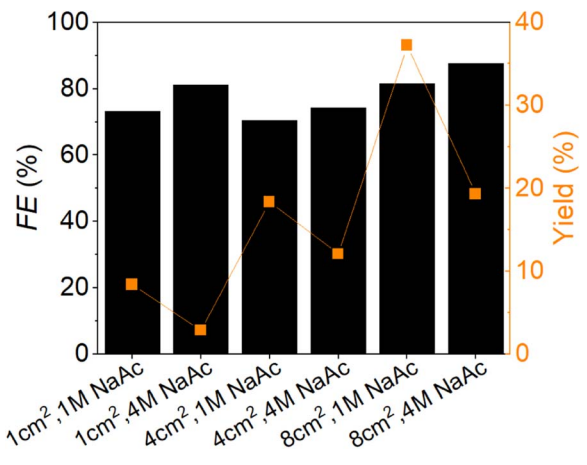

Fig. 5 Faraday efficiencies (FE) and furfuryl alcohol yields (*Y*) of the chronoamperometric experiments with different geometric surface areas of the AucAg WE and different electrolyte concentrations. The geometric surface areas for the WEs were 1, 4, and 8 cm^2. The NaAc concentrations were 1.0 (pH 8.7) and 4.0 M (pH 9.3). Reactions were conducted in an H-cell with 0.1 M furfural over a 2 h period. Ag/AgCl (saturated KCl) and platinum served as the reference electrode (RE) and counter electrode (CE), respectively.

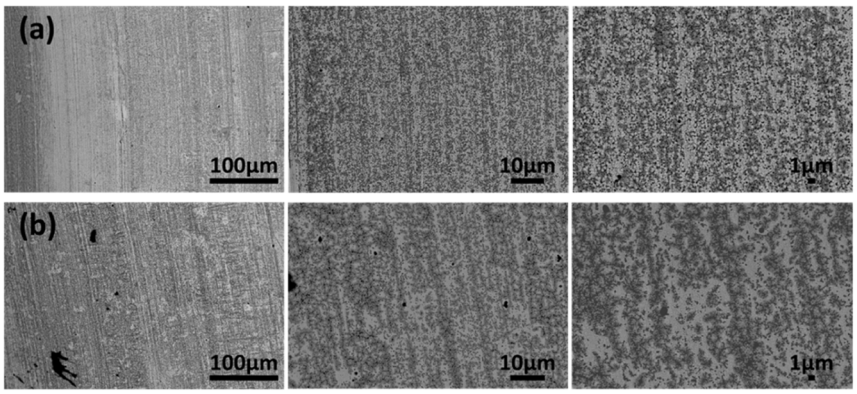

Fig. 6 SEM micrographs of the AucAg WE (a) before and (b) after the reaction with 0.1 M furfural to furfuryl alcohol. The WE had a geometric surface area of 8 cm^2 and the reaction was performed in an H-cell. The electrolyte concentration was 1.0 M NaAc and the reaction time was 2 h. A setup of Ag/AgCl (saturated KCl) was used as RE and platinum as CE, respectively. The reaction potential was set to −0.7 V *vs.* RHE (pH 8.7).

Topographical analysis *via* EDS before and after the reaction indicated no significant differences. The WE composition before the reaction was 84 wt% Ag and 16 wt% Au, while after the reaction, it was 79 wt% Ag and 21 wt% Au. The EDS spectra can be found in the ESI (Fig. S4†). Both analytical methods showed no measurable influence of the reaction and the surrounding environment on the AucAg WE. Alongside the analytical measurement methods, the chronoamperometry curve illustrates a decline in current density throughout the reaction duration (Fig. S5†). This phenomenon likely arises from diminishing reactant concentrations over time, with no evidence suggesting notable electrocatalyst inactivation.

The experimental data of this work represents a better approach in the combination of furfuryl alcohol yield (35%), FE (79%), furfuryl alcohol selectivity (54%) and with a very stable Au-coated Ag WE in comparison to previously reported studies. A more detailed comparison and discussion including a more detailed description of selected literature experiments can be found in Table S1† and the corresponding description.

Conclusions

The electrocatalytic reduction of FF to furfuryl alcohol was demonstrated as a sustainable alternative compared to the catalytic hydrogenation with H_2 gas or the Meerwein–Ponndorf–Verley approach. The electrochemical hydrogenation presents a safe process for biomass-derived production of furfuryl alcohol based on the principles of *Green Chemistry*. Various electrocatalysts were tested with multiple electrolytes *via* LSV to establish a setup for CA experiments. Acetic acid, levulinic acid, and sodium acetate were used as electrolytes based on renewable raw materials. The use of organic solvents was deliberately avoided to ensure an environmentally neutral treatment with water as a green solvent. Electrodes including Ag, Au, CP, Cu, Pt, Sn, and a gold-coated silver wire were tested. The results demonstrated a significant impact of the electrocatalytic material and the electrolyte. The best activity was achieved with gold-coated silver as the electrocatalyst and sodium acetate as the electrolyte. Optimizations involved potential screening within the range of −0.5 to −1.3 V *vs.* RHE, electrolyte concentrations between 0.1 and 4.0 M, and stirrer speeds from 0 to 1000 rpm. The influence of different alkali metal cations (Na, K, Cs) in the electrolyte, along with an increase in the WE surface area up to 8 cm^2, was also determined. Excellent electrocatalytic performance was achieved with 35% furfuryl alcohol yield and 79% FE. The optimum conditions were −0.7 V *vs.* RHE, a stirrer speed of 100 rpm, an electrolyte concentration of 1 M NaAc, and a geometric surface area of 8 cm^2 for the WE. SEM and EDS analysis indicated no significant influence of the substances on the topography and morphology of the WE during the reaction. This bioelectrorefinery concept represents an opportunity that combines biorefinery and electrocatalysis for a bio-based platform chemical. It showcases the use of renewable energy to convert furfural to furfuryl alcohol without the use of organic solvents, presenting a sustainable process.

Conflicts of interest

There are no conflicts to declare.

Acknowledgements

We would like to acknowledge the Austrian government, the provinces of Lower Austria, Upper Austria, and Carinthia, as well as Lenzing AG, for financial support. Additionally, we appreciate the contributions in kind from Johannes Kepler University, Linz, the University of Natural Resources and Life Science (BOKU), Vienna, the University of Wuppertal, and Lenzing AG. Special thanks go to our colleagues from Wood K+, Markus Huemer, as well as Erwin Malzner, Walter Milacher, and their teams, for the support in the laboratories of Lenzing AG.

References

1 M. Garedew, F. Lin, B. Song, T. M. DeWinter, J. E. Jackson, C. M. Saffron, C. H. Lam and P. T. Anastas, Greener Routes to Biomass Waste Valorization: Lignin Transformation Through Electrocatalysis for Renewable Chemicals and

Fuels Production, *ChemSusChem*, 2020, **13**(17), 4214–4237, DOI: **10.1002/cssc.202000987**.

2 Regulation (EU) 2021/1119 of the European Parliament and of the Council of 30 June 2021 establishing the framework for achieving climate neutrality and amending Regulations (EC) No 401/2009 and (EU) 2018/1999 (European Climate Law'): European Climate Law, 2021.

3 F. W. S. Lucas, R. G. Grim, S. A. Tacey, C. A. Downes, J. Hasse, A. M. Roman, C. A. Farberow, J. A. Schaidle and A. Holewinski, Electrochemical Routes for the Valorization of Biomass-Derived Feedstocks: From Chemistry to Application, *ACS Energy Lett.*, 2021, 1205–1270, DOI: **10.1021/acsenergylett.0c02692**.

4 D. S. S. Jorqueira, L. F. de Lima, S. F. Moya, L. Vilcocq, D. Richard, M. A. Fraga and R. S. Suppino, Critical review of furfural and furfuryl alcohol production: Past, present, and future on heterogeneous catalysis, *Appl. Catal.*, 2023, **665**, 119360, DOI: **10.1016/j.apcata.2023.119360**.

5 MarketsandMarkets, *Biorefinery Market by Type (First Generation, Second Generation, and Third Generation), Technology (Industrial Biotechnology, Physico-Chemical, and Thermochemical), Product (Energy driven, and Material driven) and Region - Global Forecast to 2027*, **https://www.marketresearch.com/MarketsandMarkets-v3719/Biorefinery-Type-Generation-Technology-Industrial-32837588/**.

6 Data Bridge Market Research, *Global Furfural Market – Industry Trends and Forecast to 2030*, **https://www.databridgemarketresearch.com/reports/global-furfural-market**.

7 A. O. Iroegbu and S. P. Hlangothi, Furfuryl Alcohol a Versatile, Eco-Sustainable Compound in Perspective, *Chem. Africa*, 2019, **2**(2), 223–239, DOI: **10.1007/s42250-018-00036-9**.

8 Data Bridge Market Research, *Global Furfuryl Alcohol Market – Industry Trends and Forecast to 2028*, **https://www.databridgemarketresearch.com/reports/global-furfuryl-alcohol-market**.

9 Furfural processes, in *Sugar Series : the chemistry and technology of furfural and its many by-products*, ed. K. J. Zeitsch, Elsevier, 2000, pp. 36–74, DOI: **10.1016/S0167-7675(00)80010-X**.

10 A. G. Lenzing, *Bioraffinerie*, **https://www.lenzing.com/de/nachhaltigkeit/produktion/bioraffinerie**.

11 L. Almhofer, R. H. Bischof, M. Madera and C. Paulik, Kinetic and mechanistic aspects of furfural degradation in biorefineries, *Can. J. Chem. Eng.*, 2023, **101**(4), 2033–2049, DOI: **10.1002/cjce.24593**.

12 C. P. Jiménez-Gómez, J. A. Cecilia, D. Durán-Martín, R. Moreno-Tost, J. Santamaría-González, J. Mérida-Robles, R. Mariscal and P. Maireles-Torres, Gas-phase hydrogenation of furfural to furfuryl alcohol over Cu/ZnO catalysts, *J. Catal.*, 2016, **336**, 107–115, DOI: **10.1016/j.jcat.2016.01.012**.

13 M. Jackson, M. White, R. Haasch, S. Peterson and J. Blackburn, Hydrogenation of furfural at the dynamic Cu surface of CuOCeO2/Al2 O 3 in a vapor phase packed bed reactor, *J. Mol. Catal. A Chem.*, 2018, **445**, 124–132, DOI: **10.1016/j.mcat.2017.11.023**.

14 R. V. Sharma, U. Das, R. Sammynaiken and A. K. Dalai, Liquid phase chemo-selective catalytic hydrogenation of furfural to furfuryl alcohol, *Appl. Catal.*, 2013, **454**, 127–136, DOI: **10.1016/j.apcata.2012.12.010**.

15 M. Qiu, T. Guo, R. Xi, D. Li and X. Qi, Highly efficient catalytic transfer hydrogenation of biomass-derived furfural to furfuryl alcohol using UiO-66 without metal catalysts, *Appl. Catal.*, 2020, **602**, 117719, DOI: **10.1016/j.apcata.2020.117719**.

16 M. S. Dhawan, G. D. Yadav and S. Calabrese Barton, Zinc-electrocatalyzed hydrogenation of furfural in near-neutral electrolytes, *Sustain. Energy Fuels*, 2021, **5**(11), 2972–2984, DOI: **10.1039/D1SE00221J**.

17 C. Padro and V. Putsche, *Survey of the Economics of Hydrogen Technologies*, 2010, DOI: **10.2172/12212**.

18 D. M. Alonso, J. Q. Bond and J. A. Dumesic, Catalytic conversion of biomass to biofuels, *Green Chem.*, 2010, **12**(9), 1493–1513, DOI: **10.1039/C004654J**.

19 E. Andrews, J. A. Lopez-Ruiz, J. D. Egbert, K. Koh, U. Sanyal, M. Song, D. Li, A. J. Karkamkar, M. A. Derewinski, J. Holladay, O. Y. Gutiérrez and J. D. Holladay, Performance of Base and Noble Metals for Electrocatalytic Hydrogenation of Bio-Oil-Derived Oxygenated Compounds, *ACS Sustain. Chem. Eng.*, 2020, **8**(11), 4407–4418, DOI: **10.1021/acssuschemeng.9b07041**.

20 M. Wolfsgruber, B. V. M. Rodrigues, M. G. Da Cruz, R. H. Bischof, S. Budnyk, B. Beele, S. Monti, G. Barcaro, C. Paulik and A. Slabon, Electrocatalytic Reduction of Aldonic Acids to Aldoses on Gold Electrodes, *ACS Sustain. Chem. Eng.*, 2023, **11**(1), 312–321, DOI: **10.1021/acssuschemeng.2c05576**.

21 M. G. A. da Cruz, J. N. Onwumere, J. Chen, B. Beele, M. Yarema, S. Budnyk, A. Slabon and B. V. M. Rodrigues, Solvent-free synthesis of photoluminescent carbon nanoparticles from lignin-derived monomers as feedstock, *Green Chem. Lett. Rev.*, 2023, **16**(1), 2196031, DOI: **10.1080/17518253.2023.2196031**.

22 M. G. A. da Cruz, R. Gueret, J. Chen, J. Piątek, B. Beele, M. H. Sipponen, M. Frauscher, S. Budnyk, B. V. M. Rodrigues and A. Slabon, Electrochemical Depolymerization of Lignin in a Biomass-based Solvent, *ChemSusChem*, 2022, **15**, e202200718, DOI: **10.1002/cssc.202200718**.

23 X. H. Chadderdon, D. J. Chadderdon, J. E. Matthiesen, Y. Qiu, J. M. Carraher, J.-P. Tessonnier and W. Li, Mechanisms of Furfural Reduction on Metal Electrodes: Distinguishing Pathways for Selective Hydrogenation of Bioderived Oxygenates, *J. Am. Chem. Soc.*, 2017, **139**(40), 14120–14128, DOI: **10.1021/jacs.7b06331**. Published Online: Sep. 29, 2017.

24 L. Liu, H. Liu, W. Huang, Y. He, W. Zhang, C. Wang and H. Lin, Mechanism and kinetics of the electrocatalytic hydrogenation of furfural to furfuryl alcohol, *J. Electroanal. Chem.*, 2017, **804**, 248–253, DOI: **10.1016/j.jelechem.2017.09.021**.

25 B. Zhao, M. Chen, Q. Guo and Y. Fu, Electrocatalytic hydrogenation of furfural to furfuryl alcohol using platinum supported on activated carbon fibers, *Electrochim. Acta*, 2014, **135**, 139–146, DOI: 10.1016/j.electacta.2014.04.164.

26 Bundesamt für Wirtschaft und Ausfuhrkontrolle, *Informationsblatt CO2-Faktoren:Bundesförderung für Energie- und Ressourceneffizienz in der Wirtschaft - Zuschuss*, https://www.bafa.de/SharedDocs/Downloads/DE/Energie/eew_infoblatt_co2_faktoren_2021.pdf?__blob=publicationFile&v=5.

27 F. Wang, M. Xu, L. Wei, Y. Wei, Y. Hu, W. Fang and C. G. Zhu, Fabrication of La-doped TiO2 Film Electrode and investigation of its electrocatalytic activity for furfural reduction, *Electrochim. Acta*, 2015, **153**, 170–174, DOI: 10.1016/j.electacta.2014.11.203.

28 Y. Cao and T. Noël, Efficient Electrocatalytic Reduction of Furfural to Furfuryl Alcohol in a Microchannel Flow Reactor, *Org. Process Res. Dev.*, 2019, **23**(3), 403–408, DOI: 10.1021/acs.oprd.8b00428. Published Online: Feb. 8, 2019.

29 Chemical Book, Potassium ethylate - Safety Data Sheet, *Chemical Book*, 2023.

30 J. T. Brosnahan, Z. Zhang, Z. Yin and S. Zhang, Electrocatalytic reduction of furfural with high selectivity to furfuryl alcohol using AgPd alloy nanoparticles, *Nanoscale*, 2021, **13**(4), 2312–2316, DOI: 10.1039/d0nr07676g.

31 Z. Yang, X. Chou, H. Kan, Z. Xiao and Y. Ding, Nanoporous Copper Catalysts for the Fluidized Electrocatalytic Hydrogenation of Furfural to Furfuryl Alcohol, *ACS Sustain. Chem. Eng.*, 2022, **10**(22), 7418–7425, DOI: 10.1021/acssuschemeng.2c02360.

32 H. Zhang, X. Tong, Y. Gao, H. Chen, P. Guo and S. Xue, Highly efficient catalytic valorization of biomass-derived furfural in methanol and ethanol, *J. Ind. Eng. Chem.*, 2019, **70**, 152–159, DOI: 10.1016/j.jiec.2018.10.009.

33 J. Vander Steen, F. Boissou, M. Luhmer, C. Buess-Herman, S. Baranton, C. Coutanceau and T. Doneux, Furfural electroredduction in choline-glycerol deep eutectic solvent, *J. Electroanal. Chem.*, 2023, **933**, 117269, DOI: 10.1016/j.jelechem.2023.117269.

34 N. Shan, M. K. Hanchett and B. Liu, Mechanistic Insights Evaluating Ag, Pb, and Ni as Electrocatalysts for Furfural Reduction from First-Principles Methods, *J. Phys. Chem. C*, 2017, **121**(46), 25768–25777, DOI: 10.1021/acs.jpcc.7b06778.

35 L. Almhofer, C. Paulik, D. Bammer, K. Schlackl and R. H. Bischof, Contaminations impairing an acetic acid biorefinery: Liquid-liquid extraction of lipophilic wood extractives with fully recyclable extractants, *Sep. Purif. Technol.*, 2023, **308**, 122869, DOI: 10.1016/j.seppur.2022.122869.

36 G. S. Trivedi, B. G. Shah, S. K. Adhikary, V. K. Indusekhar and R. Rangarajan, Studies on bipolar membranes. Part II — conversion of sodium acetate to acetic acid and sodium hydroxide, *React. Funct. Polym.*, 1997, **32**(2), 209–215, DOI: 10.1016/S1381-5148(96)00088-0.

37 S. Xue, C. Wu, Y. Wu, J. Chen and Z. Li, Bipolar membrane electrodialysis for treatment of sodium acetate waste residue, *Sep. Purif. Technol.*, 2015, **154**, 193–203, DOI: 10.1016/j.seppur.2015.09.040.

38 H. O. Spivey and T. Shedlovsky, Studies of electrolytic conductance in alcohol-water mixtures. I. Hydrochloric acid, sodium chloride, and sodium acetate at 0, 25, and 35 degree in ethanol-water mixtures, *J. Phys. Chem.*, 1967, **71**(7), 2165–2171, DOI: 10.1021/j100866a030.

39 S. Xue, B. Garlyyev, S. Watzele, Y. Liang, J. Fichtner, M. Pohl and A. Bandarenka, Influence of Alkali Metal Cations on the Hydrogen Evolution Reaction Activity of Pt, Ir, Au, and Ag Electrodes in Alkaline Electrolytes, *ChemElectroChem*, 2018, **5**, 2326–2329, DOI: 10.1002/celc.201800690.

40 H. Pan and C. J. Barile, Electrochemical CO2 reduction to methane with remarkably high Faradaic efficiency in the presence of a proton permeable membrane, *Energy Environ. Sci.*, 2020, **13**(10), 3567–3578, DOI: 10.1039/D0EE02189J.

41 S. Ringe, E. L. Clark, J. Resasco, A. Walton, B. Seger, A. T. Bell and K. Chan, Understanding cation effects in electrochemical CO2 reduction, *Energy Environ. Sci.*, 2019, **12**(10), 3001–3014, DOI: 10.1039/C9EE01341E.

42 M. C. O. Monteiro, F. Dattila, B. Hagedoorn, R. García-Muelas, N. López and M. T. M. Koper, Absence of CO2 electroreduction on copper, gold and silver electrodes without metal cations in solution, *Nat. Catal.*, 2021, **4**(8), 654–662, DOI: 10.1038/s41929-021-00655-5.

43 I. Szewczyk, A. Rokicińska, M. Michalik, J. Chen, A. Jaworski, R. Aleksis, A. J. Pell, N. Hedin, A. Slabon and P. Kuśtrowski, Electrochemical Denitrification and Oxidative Dehydrogenation of Ethylbenzene over N-doped Mesoporous Carbon: Atomic Level Understanding of Catalytic Activity by 15N NMR Spectroscopy, *Chem. Mater.*, 2020, **32**(17), 7263–7273, DOI: 10.1021/acs.chemmater.0c01666.

44 M. Wolfsgruber, P. Patil, C. M. Pichler, R. H. Bischof, S. Budnyk, C. Paulik, B. V. M. Rodrigues and A. Slabon, Potential dependence of gluconic acid to glucose electroreduction on silver, *Catal. Sci. Technol.*, 2023, **13**(20), 5998–6005, DOI: 10.1039/D3CY00897E.

45 Y. Seguí Femenias, U. Angst, F. Caruso and B. Elsener, Ag/AgCl ion-selective electrodes in neutral and alkaline environments containing interfering ions, *Mater. Struct.*, 2016, **49**(7), 2637–2651, DOI: 10.1617/s11527-015-0673-8.

46 Selective production of furfuryl alcohol via gas phase hydrogenation of furfural over Au/Al_2O_3.

47 Y. Zheng, Y. Jiao, M. Jaroniec and S. Z. Qiao, Advancing the electrochemistry of the hydrogen-evolution reaction through combining experiment and theory, *Angew. Chem., Int. Ed. Engl.*, 2015, **54**(1), 52–65, DOI: 10.1002/anie.201407031.

48 H. Liu, D. M. Patel, Y. Chen, J. Lee, T.-H. Lee, S. D. Cady, E. W. Cochran, L. T. Roling and W. Li, Unraveling Electroreductive Mechanisms of Biomass-Derived Aldehydes via Tailoring Interfacial Environments, *ACS Catal.*, 2022, **12**(22), 14072–14085, DOI: 10.1021/acscatal.2c03163.

49 Z. Ma, J. Chen, D. Luo, T. Thersleff, R. Dronskowski and A. Sla-bon, Structural evolution of CrN nanocube electrocatalysts during nitrogen reduction reaction, *Nanoscale*, 2020, **12**(37), 19276–19283, DOI: **10.1039/D0NR04981F**.

50 P. Krishnan and V. Biju, Effect of electrolyte concentration on the electrochemical performance of RGO-Na_2SO_4 supercapacitor, *Mater. Today*, 2022, **54**, 958–962, DOI: **10.1016/j.matpr.2021.10.512**.

51 G. E. Walrafen, W.-H. Yang, Y. C. Chu and M. S. Hokmabadi, Structures of Concentrated Sulfuric Acid Determined from Density, Conductivity, Viscosity, and Raman Spectroscopic Data, *J. Solution Chem.*, 2000, **29**(10), 905–936, DOI: **10.1023/A:1005134717259**.

52 C.-W. Sun and S.-S. Hsiau, Effect of Electrolyte Concentration Difference on Hydrogen Production during PEM Electrolysis, *J. Electrochem. Sci. Technol*, 2018, **9**(2), 99–108, DOI: **10.5229/JECST.2018.9.2.99**.

53 D. Girenko, O. Shmychkova and A. B. Velichenko, Low concen-trated green NaClO: influence of cathode material on kinetic regulari-ties of electrolysis, *Voprosy Khimii i Khimicheskoi Tekhnologii*, 2021, pp. 73–82, DOI: **10.32434/0321-4095-2021-136-3-73-82**.

54 G. K. Gebremariam, A. Z. Jovanović and I. A. Pašti, The Effect of Electrolytes on the Kinetics of the Hydrogen Evolution Reaction, *Hydrogen*, 2023, **4**(4), 776–806, DOI: **10.3390/hydrogen4040049**.

55 L. Gil-Carrera, P. Mehta, A. Escapa, A. Morán, V. García, S. R. Guiot and B. Tartakovsky, Optimizing the electrode size and ar-rangement in a microbial electrolysis cell, *Bioresour. Technol.*, 2011, **102**(20), 9593–9598, DOI: **10.1016/j.biortech.2011.08.026**.